Millimeter-Wave Phased Arrays and Over-the-Air Characterization for 5G and Beyond

Mattia Maggi, Syrine Hidri, Loic Marnat, Mauro Ettorre, Gerardo Orozco, Marc Margalef-Rovira, Christophe Gaquière, Kamel Haddadi

Millimeter-Wave Phased Arrays and Over-the-Air Characterization for 5G and Beyond

Mattia Maggi, Syrine Hidri, Loïc Marnat, Mauro Ettorre, Gerardo Orozco,

Marc Margalef-Rovira, Christophe Gaquière and Kamel Haddadi

Keywords— Millimeter-wave (mm-wave), phased arrays, beamforming, line-of-sight (LOS) over-the-air (OTA), 5G, 6G.

I. INTRODUCTION

Millimeter-wave (mm-wave) technology is a viable candidate to address the growing data traffic in fifth-generation (5G) wireless communication and beyond. However, challenges related to free space propagation loss, atmospheric absorption, scattering, and non-line-of-sight propagation must be addressed to benefit from the promised bandwidth available in the mm-wave regime. In this context, phased array technology is considered as vital to provide high-speed and seamless wireless solutions to the industry. A phased array can be defined as a multiple-antenna system that electronically controls the radiated electromagnetic beam. The official origin of the antenna array concept is attributed to Guglielmo Marconi. A repeated Morse code signal letter "S" from Poldhu, UK to St. John's in Canada was successfully demonstrated in December 1901, using a two-element antenna array. In the early 1940s, Luis Walter Alvarez designed the first electronically scanning phased-array radar. Both scientists were awarded the Nobel Prize for their discovery. Thanks to their ability to shape or steer the radiated beam and the possibility to integrate such versatile solutions in the mm-wave regime, phased arrays have shown a growing interest from the industry [2]-[8]. While these systems have been considered for decades for large radar applications and communication links, their high cost limited their penetration for commercial applications. However, the development of new architectures, packaging and semiconductor technologies has drastically reduced the cost and complexity of phased arrays making them available to commercial markets for 5G wireless and satellite applications. In particular, 5G wireless communications is bringing this paradigm to the general public.

This article presents an overview of the rise of mm-wave phased arrays in the industry including the principles and design considerations, with an emphasis on Over-The-Air (OTA) characterization. In Section II, the principle of operation and design considerations of phased array antennas are presented. A special attention is paid to phase-shifters developed in monolithic integrated technology required to control the phase profile of such arrays. The evolution toward wide bandwidth and wide scan array concepts is then proposed with connected arrays of slots and dipoles, tightly coupled dipole arrays, planar ultra-wideband modular arrays and continuous transverse stub arrays. In Section III, the OTA methodology to address the challenging task of

phased arrays characterization is described [9]-[11]. Main issues encountered in mm-wave phased array measurements are identified. Dedicated OTA set-ups for standardized and specific antenna measurements are described including a discussion about measurement uncertainty. Thanks to its high potential for 5G applications and beyond, an abundant literature related to phased arrays is reported. In the last Section, the main mm-wave applications are briefly described and future trends discussed.

II. PHASED ARRAYS PRINCIPLE AND DESIGN CONSIDERATION

A. Introduction

The available bandwidths in the mm-wave range are hindered by important atmospheric attenuation and path losses [12]. The free-space path loss ($FSPL$) can be expressed as [12]:

$$FSPL = G_{T_x} G_{R_x} \left(\frac{\lambda}{4\pi d}\right)^2 = \frac{A_e^{T_x}}{A_e^{iso}} A_e^{R_x} \frac{1}{4\pi d^2} \quad (1)$$

where $A_e^{T_x,R_x,iso}$ are the antenna physical aperture sizes of the transmitting (T_x), receiving (R_x) and isotropic antennas and d the distance between antennas in the link. Equation (1) shows that once the aperture size is fixed, the FSPL is inversely proportional to the square of the distance *d*. Typically, systems have to deal with hundreds of dB of path loss (e.g. $FSPL$ = 100 dB is reached at d = 85, 61, 40 and 25 m at 28, 39, 60 and 94 GHz respectively). Additional losses should be accounted for possible polarization mismatch due to the alignment/orientation between antennas in the link.

To overcome path losses, antennas with large gains are required to relax constraints at integrated circuits (ICs) level. Phased array antennas can offer low profile and high beam control (Fig. 1). A graphical view of the benefits of phased arrays with respect to classical isotropic radiators is shown in Fig. 1. The periodicity, lattice and radiating elements of the array are chosen to fulfil defined requirements in terms of band, field of view, radiation efficiency and cost [12]. The operation principle is based on superimposing the electromagnetic (EM) contributions of elementary sources distributed over the aperture. The resultant radiation pattern is a vector sum of the EM fields generated by each source. The effective isotropic radiated power (EIRP) of a phased array of aperture Nd^2 composed of N square elements of side $d = d_x = d_y$ can be expressed by equation (2):

$$EIRP = \epsilon_{BFN} \frac{4\pi N d^2}{\lambda^2} NP \quad (2)$$

where P is the amplified output power from amplifiers (PAs) and ϵ_{BFN} represents the losses due to the feeding network. The EIRP and directivity are proportional to N^2 and N, respectively. This means that for a fixed output power, the power amplifiers used in an array may have low gains with a benefits in terms of power efficiency, IC cost and linearity of the solution. This is key at mm-wave frequencies since the output power of solid state PAs typically drops at higher frequencies [13]-[14], motivating the increasing interest in phased arrays for 5G and beyond communication nodes.

Another advantage of phased arrays is the possibility to finely control the amplitude and phase profile over the aperture and thus the resulting radiation pattern by using the N RF accesses [15]. For 5G and beyond nodes, a directive behaviour is mainly foreseen. In those cases, the control of the amplitude mainly drives the side lobe level (SLL) and the half power beam width (HPBW) but at the expense of a lower efficiency since the PAs are not contributing at maximum to the overall output power. Phase control mainly drives the beam directions, but it can also be used to reduce/cancel out the radiation in certain directions to improve the signal to noise plus interference ratio. The multiplicity of RF accesses requires the use of a feeding network, which mainly contributes to losses in large arrays (ϵ_{BFN}). Often, an optimal number of elements can be found for a specific architecture considering the amount of gain added by elements and the increase of losses due to longer transmission lines and additional power dividers/combiners [16].

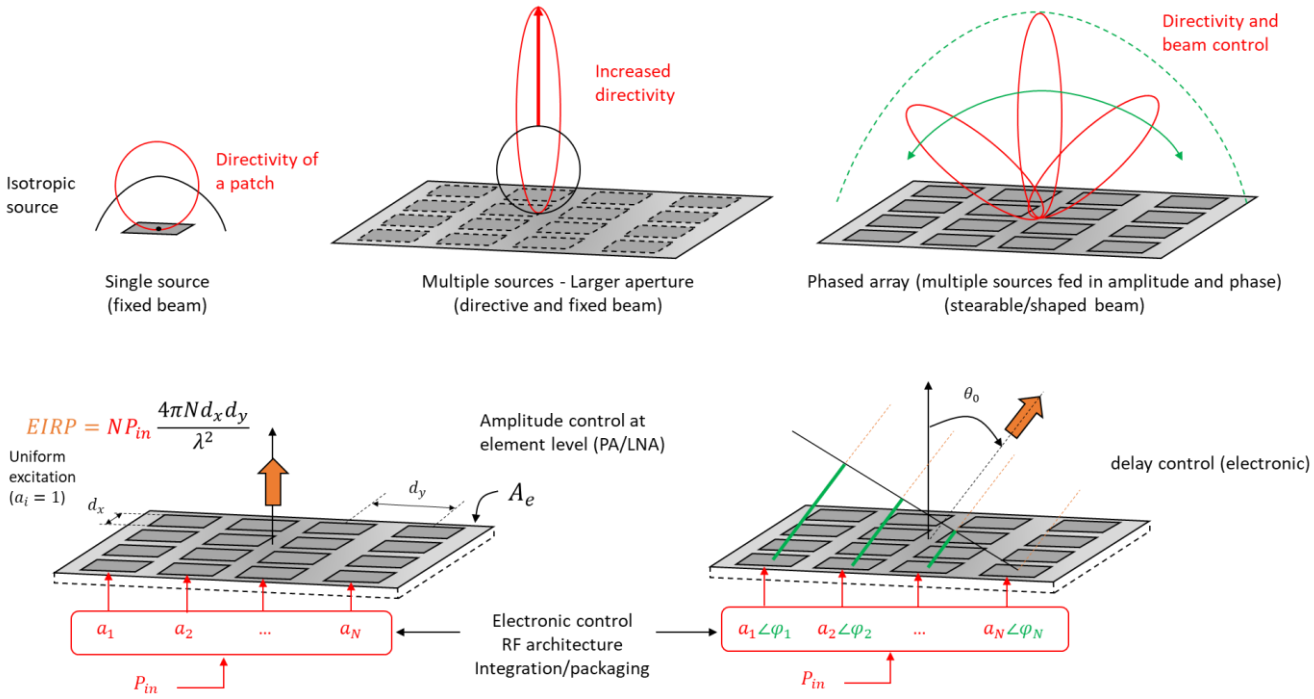

Fig. 1. Illustration of the phased array concept with directivity increase, beam control and radiated output power.

B. Phased arrays architecture and integration

For a system designer, one of the very first trade-off is to choose between analog or digital beamforming architectures based on power consumption, power management, frequency sampling, number of users, etc. [17]-[19]. Block diagrams of these two phased array architectures are presented in Fig. 2.

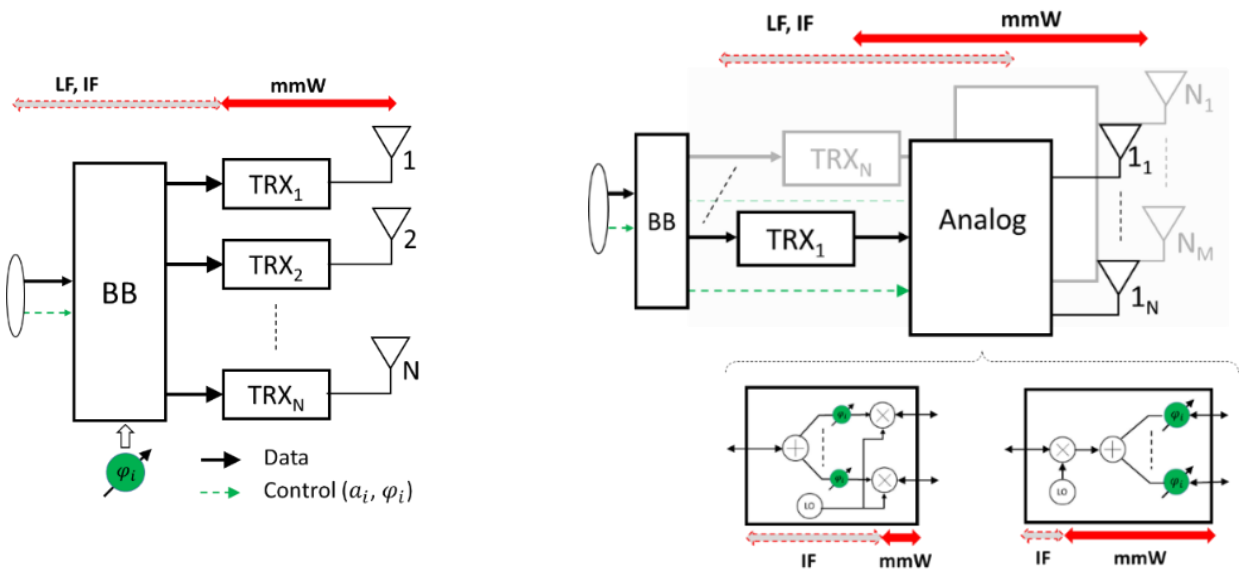

(a) (b)

Fig. 2. Block diagrams of (a) digital beamforming and (b) analog / hybrid phased array architectures; with BB: base band, transmit/receive chain (TRX), low frequency (LF), intermediate frequency (IF), local oscillator (LO).

Digital beamforming architectures (Fig. 2(a)) are characterized by an RF chain dedicated to each array element. Consequently, it can handle multiple data streams and generate multiple beams simultaneously. Digital control of the RF chains enables an optimization according to the frequency over a large frequency band. This powerful architecture requires a large number of transceivers (one per antenna) and A/D converters, and its performance may be affected by RF impairments [20].

In analog beamforming architectures (e.g. single RF chain in Fig. 2(b)) on the other hand, the analog signal is generated by one RF chain and applied to all array elements through amplitude/phase variation devices. Analog beamforming in the RF path is simple and uses a minimal amount of hardware. One advantage of using analog architectures is the ability to cancel out spatial interferences signal (spatial filtering before mixers), unlike in digital beamforming where the interference is impinging on all array elements without pattern cancellation (spatial filtering after mixers) decreasing the signal to noise ratio.

Hybrid architectures (e.g. multiple RF chains in Fig. 2(b)) are offering a modular approach consisting of scalable phased arrays. It has less degrees of freedom as compared to digital baseband processing and less simultaneously supported streams, but it results in a significant reduction of the cost and the power consumption. This architecture can also improve yield and robustness of the overall antenna.

Depending on the architecture, the amount of functions to be included at the IC level may lead to a large chip area. Above 40 GHz, the IC dimensions become similar to the array radiating element making its integration critical. This may lead to increase inter-element spacing or use a cluster topology (multiple elements fed with same amplitude and phase) both reducing the scanning capability of phased arrays. The way to separate the functions in the architecture affects the complexity and cost

of the package [18], [21]. The packaging definition has to account for (i) radiating element design (number of layers and precision), (ii) size and number of I/O (Input/Output) of the IC, (iii) size of the array/tile, (iv) number of layers to route mm-wave, intermediate frequency (IF), digital I/O or control signals, and (v) power supply and potential passive components. The phase shift is also affected by the architecture and can be applied to the baseband signals or at the local oscillators (LO) level (not represented). Alternatively, to reduce the transceiver size, complexity and power consumption, the phase shift can be applied to the RF/mm-wave signals.

C. Phase shifters in integrated technologies

With phased arrays featuring large number of radiating elements (e.g., [22]) silicon-based technologies (i.e., generally CMOS or BiCMOS) are considered as one of the most cost-effective solutions for the design of these devices. Phase shifters can be built as active or passive devices. A passive phase shifter refers to a device whose energy consumption is not used for amplification purposes, hence leading to far lesser power consumption than its active counterparts, which perform signal amplification.

Active phase shifters are typically based on the vector-sum principle (i.e., combining two RF signals with different phases and magnitudes). It usually uses variable-gain amplifiers (VGAs), appearing as a very interesting option, as they combine the amplification and phase shifting functions in a single block. In addition, this kind of phase shifter can control the amplitude of the output signal. However, the phase coverage of these devices depends on the synthesizable gain difference between the embedded amplifiers and phase difference between input signals. Hence, when targeting large phase shift coverage, several VGAs are required [23]-[25], leading to large power consumption. In addition, these kind of phase shifters usually suffer from narrow bandwidth and linearity issues, which require designers to use additional linearization techniques [25]. Another solution is the use of True Delay Units (TDUs) [26]-[28] to increase the bandwidth of active phase shifting architectures ensuring a perfect control of the beam orientation over frequency (beam squint issues [12, 16]), at the expense of a more complex architecture.

On the other hand, passive phase shifters can mainly be divided in three categories: (i) switched-type, (ii) loaded-type and (iii) reflection-type. *Switched-type phase shifters* [29]-[31] use switching elements (e.g., transistors or diodes) to choose among several signal paths presenting particular phase shifts. This kind of phase shifters can be designed using lumped elements (i.e., capacitors and inductors). Switched-type phase shifters present a discrete number of achievable phase shifts that depends on the number of cells they contain. Thus, the main drawback is their area overhead when aiming at fine phase shift steps. In addition, at mm-waves, switches introduce important losses of around 1.5 to 2 dB per switch [32], [33]. The *loaded-type phase shifters* can be built using lumped elements or transmission lines [34], [35]. The phase at the output is usually modulated in a continuous manner using integrated varactors. Switching elements such as MOSFETs or PIN diodes can be used to switch between a set of reactances resulting in a discretized output phase shift [36]. Even though these devices present a simple and compact solution

for their integration, they usually suffer from poor return loss and limited phase shifting range. The last kind of widely used integrated phase shifters is the so-called *reflection-type phase shifters (RTPS)* [37]-[39]. These phase shifters are composed of two blocks: (i) a 3-dB quadrature coupler and (ii) a highly-reflective load placed at the coupled ports of the coupler. These phase shifters, when integrated with a highly-directive coupler have the advantage of presenting return loss close to the directivity of the used coupler for any load impedance. For this reason, this system can present low return loss over a wide frequency band of operation. In addition, they allow a continuous phase tuning. However, the design of high-performance integrated 3-dB couplers and varactors remains a challenge at mm-wave frequencies.

D. Phased arrays for 5G applications: focus on V-band for the access point and back/front haul

In Fig. 3, a non-exhaustive list of commercial phased array solutions operating over 28 to 60 GHz bands is reported [40]. As can be seen, both user equipment and access point applications are covered. The first mm-wave phased array solutions available were focusing on the unlicensed V-band for short range and high data rate wireless links. Recently, solutions have been proposed with larger EIRP, 60-element array or more and extended scanning range of ± 45-60°.

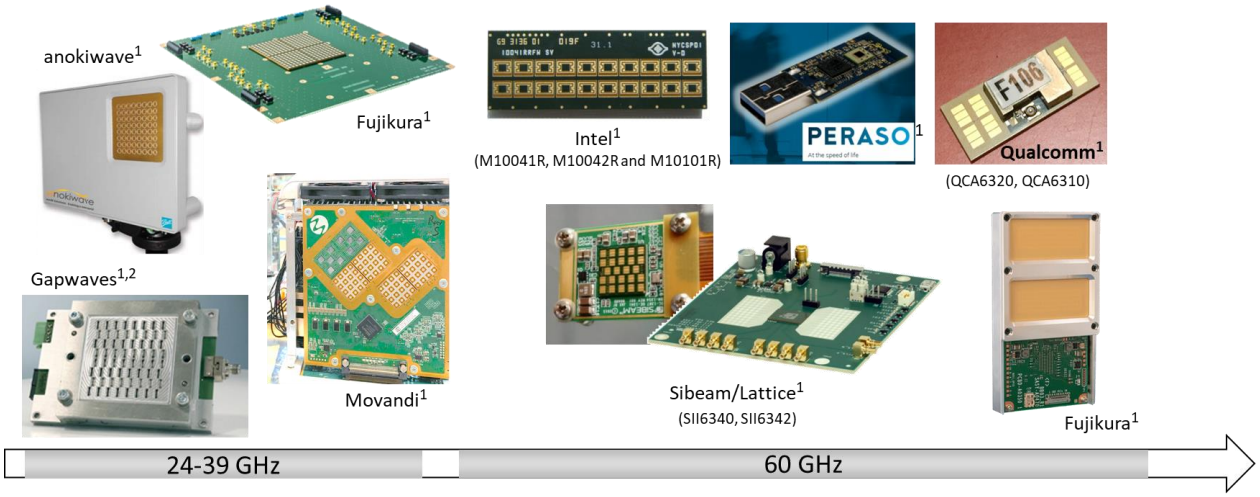

Fig. 3. Commercial phased arrays solutions [40]. ([1] oriented toward communication applications; [2] oriented toward radar applications)

A lot of effort has been done to improve performance and compactness of mm-wave phased arrays [18], [41], [42]. Photographs of the main silicon based prototypes operating in the main 5G mm-wave frequency bands proposed these last years are depicted in Fig. 4. Three main strategies have been considered for the packaging of the active phased array prototypes:

- *Single chip phased array*: In this configuration, large silicon chips are composed of all functions from low frequency to mm-wave signal and are perfectly scalable. To reach large number of RF access, multiple ICs are joint at wafer level. In [43], a novel technique that requires only one fabrication cycle to build any phased-array size is proposed.

Two packaging topologies are considered. First, the antenna elements are designed on a low loss quartz substrate, taking the advantage of microelectronic material and processes, and excited by EM coupling from the 64 and 256 on-chip feeds [43-44]. In the second approach, the phased array relies on the assembly of a large RFIC chip (joint 4 chips) on a low cost organic-based multi-layered module (16 layers) integrating 64 active antennas [45].

- *Multi-chip / single board phased array*: In this solution, the substrate used to design the antenna array is also used to integrate multiple chips. One of the main advantage is that large antenna arrays can be designed with an easy and reliable process to assemble the chips and the rest of the electronic. This is particularly true when the minimum feature size required to route and assemble the active phased array is far from the limit of the packaging technology. This is why most of the prototypes below 40 GHz use such an approach with printed circuit board (PCB) or organic technologies [46]-[50]. In [21], the authors highlighted the issue to fit beam former ICs below the antenna elements at 60 GHz. At 94 GHz, the same issue rises for a 64-active-element module proposed by [51], where 36 dummy elements had to be added. The main drawback of this solution is the lack of scalability that requires a redesign of the phased array to scale it up or down.
- *Multi-chip / multi-tile phased array*: The main advantage of this approach is to reach any phased array dimensions simply by using one or multiple tiles without additional antenna design effort. The tile approach requires more aggressive packaging technology to route all signals (RF, control, power supply) while keeping the scalability of the solution. In [52], 12 metal layers have been used to co-package four ICs on a $8.1\times7.5\text{mm}^2$ module. At higher frequencies, the constraints become more stringent and in [41], the physical constraints set by the RFIC and the PCB process lead to widen the inter-element distance to 0.63λ (2.1 mm) reducing the maximum scanning capability at 90 GHz. Nevertheless, the solution remains scalable. Preliminary results of a phased array on PCB technology operating at D-band has been presented in [53] but is extremely constrained. Future high mm-wave bands phased array may benefit from the use of more aggressive packaging technology (often limited in term of maximum module size) to further reduce the array spacing, improve IC integration and ensure scalability.

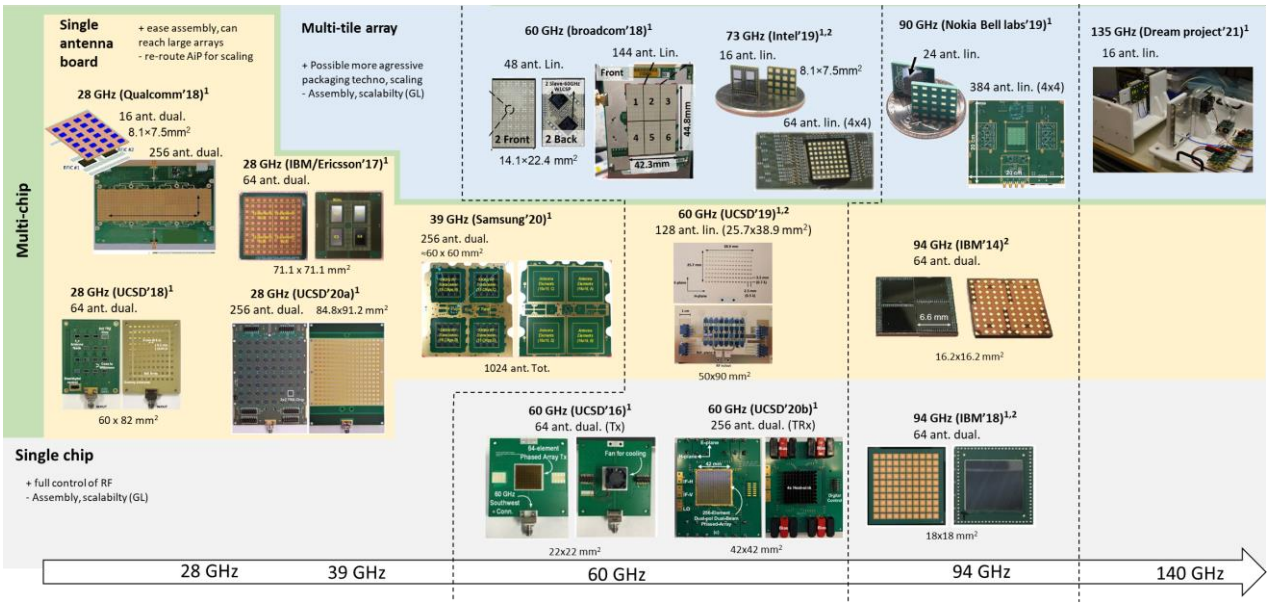

Fig. 4. Integrated silicon based phased array antenna solutions.

(Qualcomm'18 [46][1], UCSD'18 [48][1], IBM/Ericsson'17 [47][1], [44], UCSD'20a [49][1], Samsung'20 [50][1], broadcom'18 [54][1], UCSD'16 [43][1], Intel'19 [52][1,2], UCSD'19 [21][1,2], UCSD'20b [44][1], Nokia Bell labs'19 [41][1], IBM'14 [51][2], IBM'18 [45][1,2], Dream project'21 [53][1]). ([1] designed for communication applications; [2] designed for radar applications)

The previously presented phased arrays prototypes show performance in accordance with their targeted applications. However, for upcoming 5G and beyond applications, fully integrated front-ends compatible with much wider bandwidth (>20%) and scanning capabilities (>±45°) will be needed with major challenges for the antenna design. The combination of non-resonant radiating elements and a perfect control of the mutual coupling between array elements over frequency and scanning range can pave the way to innovative designs to overcome typical limiting factors such as scan blindness, limited bandwidth, high reflections, limited field of views, etc. [12, 16]. The next section provides an overview of antenna concepts that may fill this gap and enable unprecedented functionalities for 5G and beyond applications.

E. Wideband and wide scan arrays

The principle of operation of wideband and wide scanning arrays consists in creating a continuous current distribution over the radiating aperture to avoid resonances and reduce impedance variations at the array elements over frequency and scan range[55]. Among the different implementations, connected arrays of slots or dipoles, tightly coupled dipole arrays (TCDA), Planar ultra-wideband modular array (PUMA) and continuous transverse stub (CTS) arrays are the most popular. In the following, these architectures are described, and main performances are summarized.

1) Connected arrays of slots or dipoles

Connected arrays consist of slots or dipoles fed at the Nyquist interval (half wavelength at the highest frequency of operation). In [56], a backing reflector plane, spaced at a quarter wavelength away from the radiating aperture was introduced to achieve unidirectional radiation at the expense of the operation band and scanning capabilities [57], [58]. Artificial dielectric

layers (ADLs), realized with relatively small metal patches, were introduced to ease the impedance matching of the array and allow a smaller distance between the ground plane and the radiating aperture. Arrays with relative bandwidths as large as 30 to 85% have been reported for a field of view in elevation of about ±60° in all azimuthal planes [59], [60]. The current research effort focuses on the fabrication of such arrays in planar technologies to further reduce their profile and still achieve wider bandwidths and field of views [60]. A graphical representation of the evolution over time of such arrays is illustrated in Fig. 5.

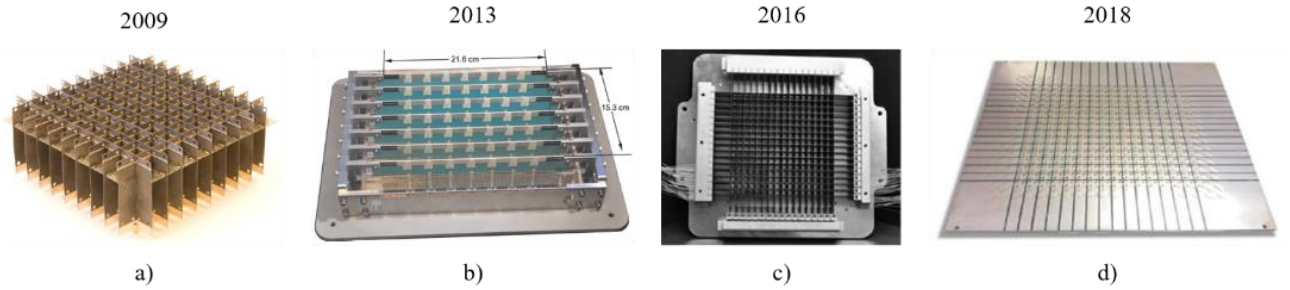

Fig. 5. Technology evolution of connected arrays ((a) 8x8 elements, BW: 40%, Scan: ±45°, vertical PCB [61]; (b) 7x7 elements, BW: 50%, Scan: ±45°, vertical PCB [57]; (c) 16x16 elements, BW: 40%, Scan: ±60°, vertical PCB [58]; (d) 16x16 elements, BW: 86%, Scan: >±60°, multi-layer planar PCB [59]).

2) Tightly Coupled Dipole Arrays (TCDA)

TCDA stems from the original concept by Prof. Munk namely the current sheet array (CSA) [62]. As for connected arrays, the main technological challenge has been to properly match the array while preserving their bandwidth and field of view. In particular, the array matching has been achieved by resorting to different types of baluns with final bandwidth as large as 10:1 [63], [64]. The reduction of the profile of the antenna has followed similar approaches of connected arrays by introducing a wide angle impedance matching (WAIM) layer made by frequency selective surface (FSS) located above the radiating aperture. Field of view larger than ±60° in the principal planes [65]-[68] have been reported during the years.

3) Planar Ultra-wideband Modular Array (PUMA)

The PUMA architecture is based on capacitively coupled radiating dipoles. The main features of this technology are very low profile and size modularity. The radiating dipoles are printed on thin dielectric layers and a WAIM layer is added above to improve the matching properties. Field of views as large as ±60° in elevation have been reported over bandwidth as wide as 6:1 [22]-[71]. Such structures are suited to multi-layer PCB technology. As for the previous cases, the actual challenges are to further reduce the complexity of the feeding system at the array element level while preserving scanning range, bandwidth and cross-polarization purity.

4) Continuous Transverse Stub arrays (CTS)

CTS arrays are composed of long slots fed [72] generally by a quasi-optical system through a corporate feednetwork. One or several feeds are located in the focal plane of the quasi-optical system to achieve scanning along a plane parallel to the radiating slots by switching between them. As a difference with respect to the previous concepts, the main beam can be only steered along one principal plane. Scanning as wide as ±45° in elevation have been reported in the full Ka-band [73]. The mechanical rotation of the entire antenna is then required to cover other azimuthal planes. During the years, the concept has been implemented with various technologies [74]. Current research focuses in planar fabrication technologies such as LTCC (Low-Temperature Co-fired Ceramic) and PCB [75], [76] and to further extend the capability of the antenna in terms of band and scanning range.

A brief overview summarizing the capability of such array concepts in terms of bandwidth, polarization agility (Pol.), cross-polarization (X-pol.), active VSWR (Voltage Standing Waves Ratio) and radiation efficiency η (estimated values are derived as the ratio between antenna gain and directivity when the effective radiating aperture is uniformly illuminated) is reported in Table 1. It clearly appears that such arrays can achieve very large bandwidth with scanning larger than ±60° and polarization agility enabling performance unachievable by classical antenna array concepts (section II.D).

Table 1. Wideband and wide scan array concepts performance.

Ref.	Bandwidth [GHz]	Scan Range	Pol.	X-pol. [dB]	Active VSWR	Thickness	η
Connected Array 2018 [59]	2.5:1 [6 - 15]	>± 60°	Double	<−6 (E-H-D-planes)	<3.2 (E-H-planes)	$\sim 0.55\lambda_{high}$	-
TCDA 2020 [67]	46:1 [0.13 - 6]	± 60°	Double	<−12 (E-H-D-planes)	<4 (E-planes)	$\sim \lambda_{low}/13.5$	~ 72%**
TCDA 2020 [68]	12:1 [0.19 - 2.3]	± 60°	Double	<-20 Suppr. From Co-pol.	<5.5 (E-H-planes)	$\sim \lambda_{low}/10$	28%*
PUMA 2018 [71]	6:1 [3.53 - 21.2]	± 60°	Double	<−10 (E-H-D-planes)	<3.8 (E-H-D-planes)	$\sim 0.48\lambda_{high}$	~ 95%**
CTS 2018 [75]	[57 - 66]	± 38°	Single	<−8 (E-H-planes)	-	$\sim 0.9\lambda_{high}$	-

Radiation efficiency: *Estimated; **Measured.

This section introduced current state-of-the-art phased array topologies, describing the main antenna and phase shifter architectures. New antenna array topologies enabling ultra-wide bandwidth and field of view have also been introduced. Phased arrays, as any other electronic device, require characterization to ensure that they operate within the expected specifications. In the following section, over-the-air (OTA) characterization is described together with the most relevant metrics for phased array systems.

III. OVER-THE-AIR (OTA) CHARACTERIZATION MEASUREMENTS

The standard technique to determine radio performance in wireless systems is known as OTA characterization. In the first part of section II, it has been shown how phased array antennas are versatile in radiated power and radiated beam shaping. To properly characterize them, OTA measurements must account for these specific and dedicated needs. A focus on OTA measurements, specifically for wireless industry, is presented in this section. The general OTA architecture is presented with related set-up modification to achieve the specific application needs. The measurement uncertainty of the OTA set-up, including the major contributions, are given to quantify the performance of the OTA method based on 3rd Generation Partnership Program (3GPP) [81]. Finally, a prospective view related to major challenges with a focus on massive production and commercialization of the devices in the industry is described.

5G mm-wave tests depend mainly on massive MIMO technology in which phased array antennas replace antennas used in previous generations of mobile communication. OTA testing is required for two main reasons. On the first hand, conventional RF probing techniques (on-wafer or coaxial) are not possible due to the lack of mm-wave probe connectors or dedicated footprints. Indeed, in 4G, dedicated PCB footprints are available in all designs to connect an RF probe to the RF test instrumentation. On the second hand, as phased arrays antennas radiate at different time intervals, free-space characterization is required to test the overall combined performance of multiple antennas.

The requirements on RF characterization methods differ fundamentally with 5G mm-wave applications. Indeed, regarding previous generations of mobile networks, characterization of both radio and antenna parts were performed independently. Once they were both understood, a simplified end-of-line test was performed in production. With mm-wave, both beamformer and antenna can be tested individually, but the overall performance can vary once those two components are assembled. Consequently, 3GPP conformance test has to be done over the air.

The design cycle of the phased array antenna involves different types of instrumentation. Once the design is ready, different building blocks need to be characterized and validated. During the design process, each individual single element is measured and understood to the fullest using traditional antenna theory and measurement [77]. The critical testing phase is the Verification and Validation (V&V) of the full device where a full characterization is required. In production, a subset of the V&V is usually executed but with the mindset to find manufacturing errors vs understanding the performance of the device. Key measurements to perform on phased array antennas for the mm-wave 5G market are divided in two types of measurements:

1. Antenna specific measurements:
    a. Continuous waveform (CW) stimulus.

b. Effective Isotropic Radiated Power (EIRP): in general, it refers to the radiating power in a specific location of a spherical surface around the antenna compared to an isotropic radiator at the center of the same sphere.

c. Total Radiated Power (TRP): the integration of all the EIRPs around the spherical surface determines the total radiated power emitted by the antenna.

d. Beam characteristics: beam width, sidelobes power, first null location, etc.

2. Standards measurements (based on 3GPP [78], [79] and the US Cellular Telecommunications and Internet Association (CTIA) [80]):

    a. Modulated 5G New Radio signals as stimulus.

    b. EIRP and TRP.

    c. Modulation Accuracy.

    d. Adjacent Channel Leakage Ratio (ACLR) or Adjacent Channel Power (ACP).

    e. Spectral Emissions.

    f. Effective Isotropic Sensitivity.

The following part is focusing on the commonality of the measurements rather than the differences. Most of them capture the directional feature and agility in reconfiguration of phased array. At the same time, they also provide the metrics of the wireless link within the a network. The 3GPP measurements are an extension of the extensively documented measurements procedures described in previous cellular standards and are well documented in [82]. The new concept in New Radio for phased array antennas is the EIRP and TRP antenna concepts described in the following. An example of measurement system using a typical test setup is described for better understanding in Fig. 6.

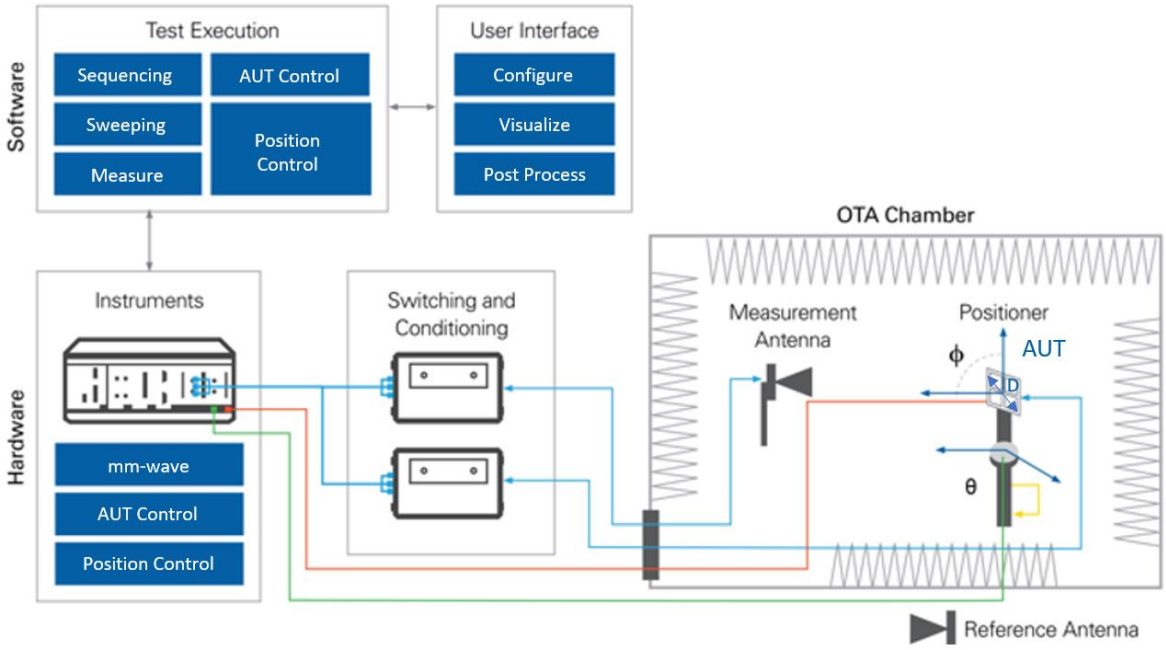

Fig. 6. Overview of an OTA setup for phased array antennas testing.

Either the Antenna Under Test (AUT) or the Measurement Antenna moves in spherical coordinate systems with the angles θ (elevation) and φ (azimuth) as represented in Fig. 6. For each position, a measurement using a Measurement Antenna (also called Probe Antenna) is taken. This mean that each seta of measured data is function of (θ, φ). This process is done with dual-polarized antennas and thus we also have a third variable which can be V or H polarization. Total Radiated Power (*TRP*) is defined as:

$$TRP = \frac{1}{4\pi}\int_0^{2\pi}\int_0^{\pi}\left(EIRP_V(\theta,\varphi) + EIRP_H(\theta,\varphi)\right)sin\theta d\theta d\varphi \quad (5)$$

Modulated measurements in the 5G New Radio standard are also dependent on spatial variables. For example, Adjacent Channel Power (ACP) requires to measure the *TRP* of the main channel and then the *TRP* of each adjacent channel. Therefore, to fully characterize the phased array, the positioner needs to move into multiple discrete (θ, φ) and then collect all measurement data (spatial sampling). This can be a long process depending on the number of (θ, φ) to be assessed. Given that phased array antennas have high directivity, the number of grid points needs to be large enough as explained in Table II where the accuracy of EIRP depends on the number of grid points:

Table II. Trade-offs between test time (based on 120 ms movement and 30 ms measurement) and accuracy. The mean error is based on [84] for a simulated 8x2 array widely used in 3GPP.

No. of grid points (constant step size)	Test time (s)	EIRP Mean error (dB)
6000	900 s (15 min)	0.02
800	120 s	0.2

200	**30 s**	**0.74**

This error will be important when making decisions on the Measurement Uncertainty (MU) needed for the test. This measurement error is discussed later.

The OTA system to characterize mm-wave phased arrays consists on a signal generator (to generate stimulus signal) capable of doing modulated as well as CW measurements and a Signal Analyzer capable of demodulating wideband signals. In the Transmit (Tx) test, the stimulus goes to the AUT. The radiated signal from the AUT is captured by a Measurement Antenna connected to the Signal Analyzer. In a Receiver (Rx) test, the Signal Generator radiates using the Measurement Antenna while the AUT receives the signal processed to the Signal Analyzer to determine the measurement performance. Both Tx and Rx can be configured using the same setup by adding external switching devices.

One important concept in OTA systems is the distance between the Measurement Antenna and the AUT. This distance is critical as: being too close, the radiation pattern is not yet formed; and being too far, the energy in the area received by the Measurement Antenna is reduced according to the path loss equation (1). The distance should be guided by the aperture D of the AUT (Fig. 6). The far-field (Fraunhofer) distance is defined as $\frac{2D^2}{\lambda}$. At this distance, a phase difference between the edge of the aperture and the center is 22.5°[12]. The simplest method called direct far field (DFF) is to directly place an antenna in the far-field region and perform the measurements. In this measurement configuration, the largest drawback is attributed to the path loss that increases with distance, according to (1). Consequently, operating in the far-field region has a direct impact on the link budget. For example, for the user equipment (UE), an error vector magnitude (EVM) of better than -22 dB is required at the lowest EIRP which is set to –6 dBm for 64 QAM [79]. An example of link budget in an OTA setup is given in Fig. 7.

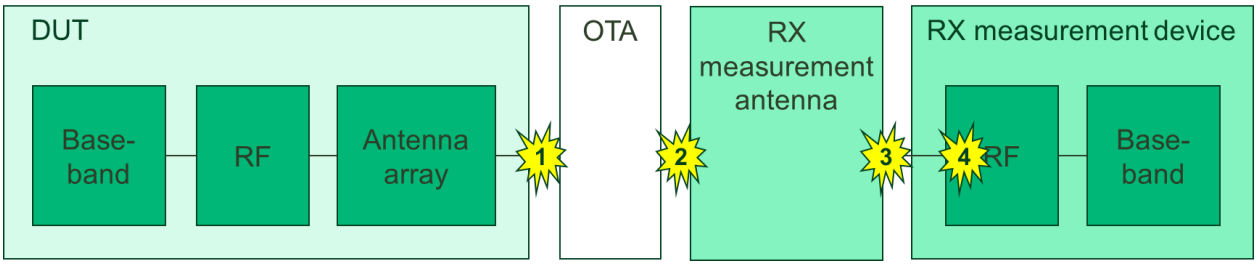

Fig. 7. Link Budget of OTA. Considering an antenna array of 5 cm aperture with –6 dBm output EIRP (1) as minimum requirement, a path loss of 57 dB (0.62 m of far field distance at 28 GHz) bringing the signal down to -63 dBm (2). Assume the Measurement Antenna has 15 dBi of gain so -48 dBm at (3). Assume some losses on the cables to the instrument. This signal noise can be New Radio 100 MHz or 80 dB of noise. Assuming the instrument has 10 dB of noise figure (NF), this means that the noise at the instrument is -174 dBm/Hz + 10 dB + 80 dB = -84 dBm. The best possible SNR of the signal is 36 dB and when testing phased array antennas, it requires to be 8-10 dB better than the specification of 22 dB EVM. This means, cable losses cannot exceed 4-6 dB in this fairly ideal scenario.

Antenna-in-Module (AiM) devices with just few elements and antenna apertures below 5 cm benefit from a Direct Far-Field (DFF) approach that preserves link budget and ensures testing with greater signal-to-noise ratios (SNR). However, testing system-

level designs with a larger number of antenna elements and antenna apertures above 5 cm requires an indirect far-field (IFF) approach (also called Compact Antenna Test Range - CATR) that produces a high-quality Quiet Zone (QZ) with minimal phase and amplitude variation (typically ± 5° and ± 1.5 dB), following the 3GPP specifications for IFF testing (Fig. 8).

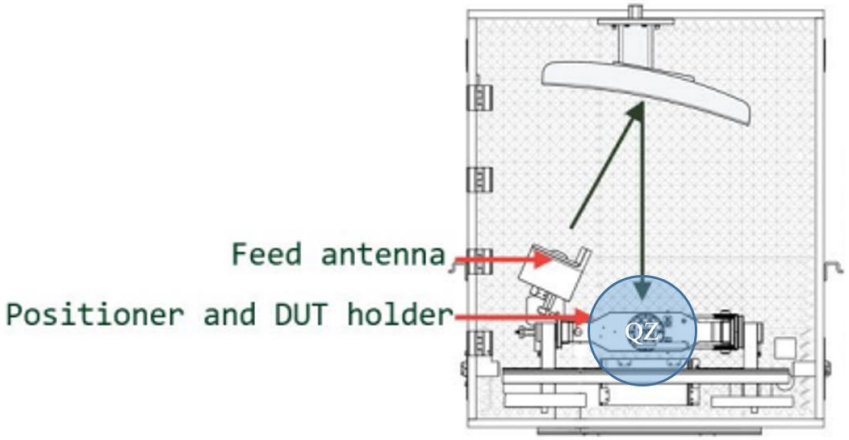

Fig. 8. Compact Antenna Test Range (CATR) setup.

A CATR system has the advantage to create a homogeneous QZ that is large enough to include multiple smaller phased arrays (e.g. UE) or one large phased array (e.g. Small Cells or Customer Premise Equipment) while keeping the path loss much smaller as compared to a DFF system. The path loss can be accurately estimated in the full system with a proper methodology [85].

The final method approved by 3GPP is near field probing. This one consists of sampling the E-field at close proximity of the AUT. The difficulty here is to avoid any antenna coupling and any reflections that will modify the antenna behavior. The other difficulty is that the current near field to far field transformation methods should be adapted to modulated measurements.

The last element of OTA measurements is the accuracy or Measurement Uncertainty (MU). Each setup described previously has multiple contributors for MU and below we list the ones that contributes the most for a specific measurement. Fig. 9 presents the MU budget for the Peak EIRP power.

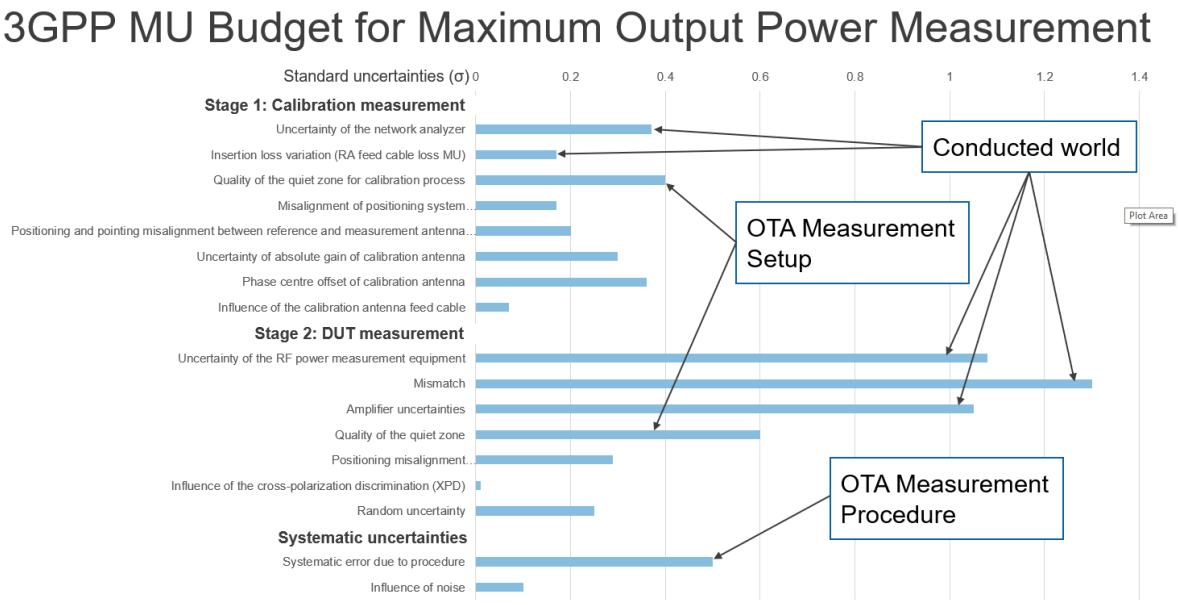

Fig. 9. Maximum output power MU budget. Total measurement uncertainty (a squared root of the sum of squared of the individual values) ~ 5 dB (coverage k = 1.96, 95% level of confidence) from [81], [86].

The main critical areas related to OTA measurements are summarized in the following points:

- The Quiet Zone (QZ) is the area where power and phase variations of the generated field are minimized. In these conditions, the far-field conditions are approximated and therefore, the AUT must be positioned inside this volume also shown in Fig 8 (blue circle area).
- The measurement of the quiet zone is challenging at mm-wave, in particular with high directivity mm-wave antennas. The 3GPP method is listed in [81]. More holistic methods have been proposed [87], but from commercial point of view, the cost is still too high to be widely adopted.
- The number of grid points was pointed out in Table II where the MU is systematically added (no square-root of the sum) to the budget, making it an important consideration to reduce the overall MU.
- AUT positioning is the other important consideration as any error of position might not affect much the amplitude but may significantly affect the phase (1 mm at 30 GHz corresponds to 36°).
- Finally, 5G devices may have more than one mm-wave phased array antenna. In this case, it is important to consider antenna placement since for of the center antennas there will be multiple geometric errors as illustrated in Fig. 10(a). This is especially important if the AUT is a multi-antenna device [Fig. 10(b)].

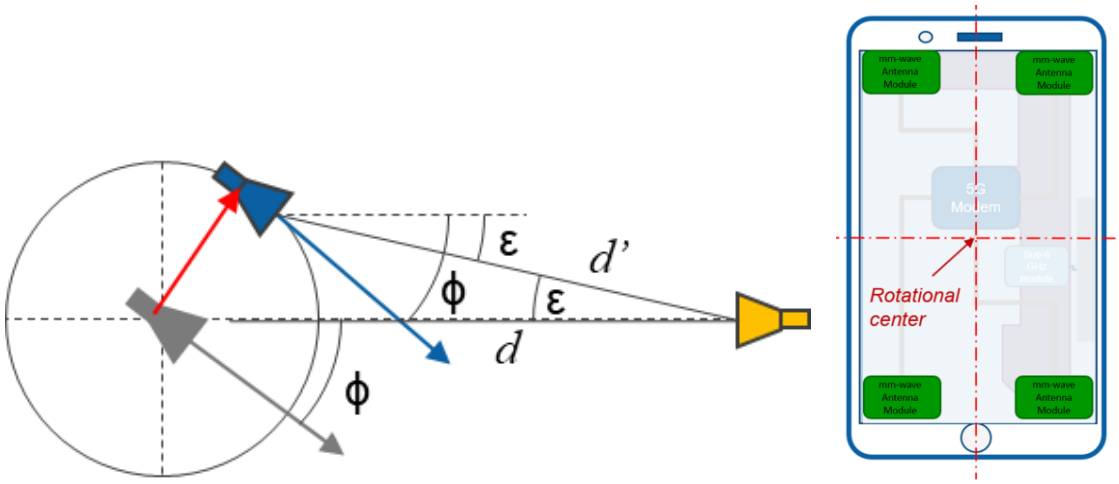

(a) (b)

Fig. 10. (a) Geometrical errors when a single AUT is not at the exact center of rotation and (b) Case of a multi-antenna device.

To test the phone in Fig. 10(b), each antenna needs to be placed at the center of the positioning system. Therefore, a repositioning of the device is required for each tested antenna. To avoid such time consuming operation, the Quiet Zone shall be large enough to include all antenna positions of device under test. This is called the black box approach where the location of antennas is not known and thus the quality of the Quiet Zone is critical to compare the performance between the different antennas on the device.

This section has shown the various variables and challenges that are presented when trying to characterize phased arrays over-the-air. The main challenges of capital cost, MU and test times is constantly changing to make possible a full commercialization of these mm-wave phased array antennas for 5G. In the last section, we present briefly 5G applications and future trends foreseen by industry and academia.

IV. CHALLENGES & FUTURE TRENDS FOR 5G AND BEYOND

In the field of mobile 5G communications, high data rates up to 10 Gbps and low latency of less-than-1ms are required to address real-time new applications such as machine to machine (M2M), Internet of vehicles (IoV), device to device (D2D) [87]. To achieve 1000× capacity increase over 4G, three key technologies have been identified [88]: mm-wave mobile broadband [89], massive multiple-input multiple-output (MIMO) [90], and small cells [91]. These technologies are combined with phased array technology to enhance the wireless link performance. Whereas beamforming techniques in the mm-wave regime using integrated circuits have been exemplary demonstrated with multi-Gb/s data transmission capability, mobile devices have strong requirements in terms of compactness, cost and power consumption [92] (Fig. 11). In mobile devices, only a few of mm-wave antennas can be embedded whereas hundreds of antennas can be embedded in 5G base stations. In contrast with sub-6 GHz frequencies, severe free-space signal attenuation at mm-wave range have directed the efforts to develop silicon semiconductor

circuits and integrated chips associated to large-scale mm-wave phased arrays and beam switching antennas to maximize both the antenna and amplifier gains and consequently enhance 5G wireless link budget [93]-[94].

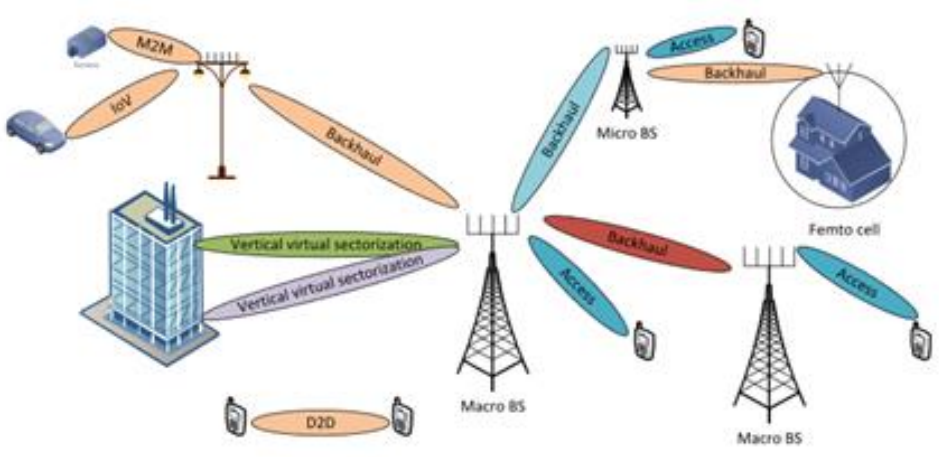

Fig. 11. MM-wave massive MIMO beamforming in 5G wireless protocols [92].

In the space sector, phased array technology has been identified as viable solution to meet future systems requirements in terms of increasing number of nodes,shared spectrum and reconfigurability. In particular, phased array antennas present features such as high gain, long distance coverage, agile and rapid beam-steering together with multi-beam capabilities. The first marine satellite SEASAT-1 based on active phased array antenna technology was successfully launched by NASA in June 1978 [96]. Since then, the technology has known a continuous and growing interest with satellites equipped with active phased arrays antennas [95]-[97] (Fig. 12). More integrated and light weight technology considering spatial constraints would open new perspectives for space applications .

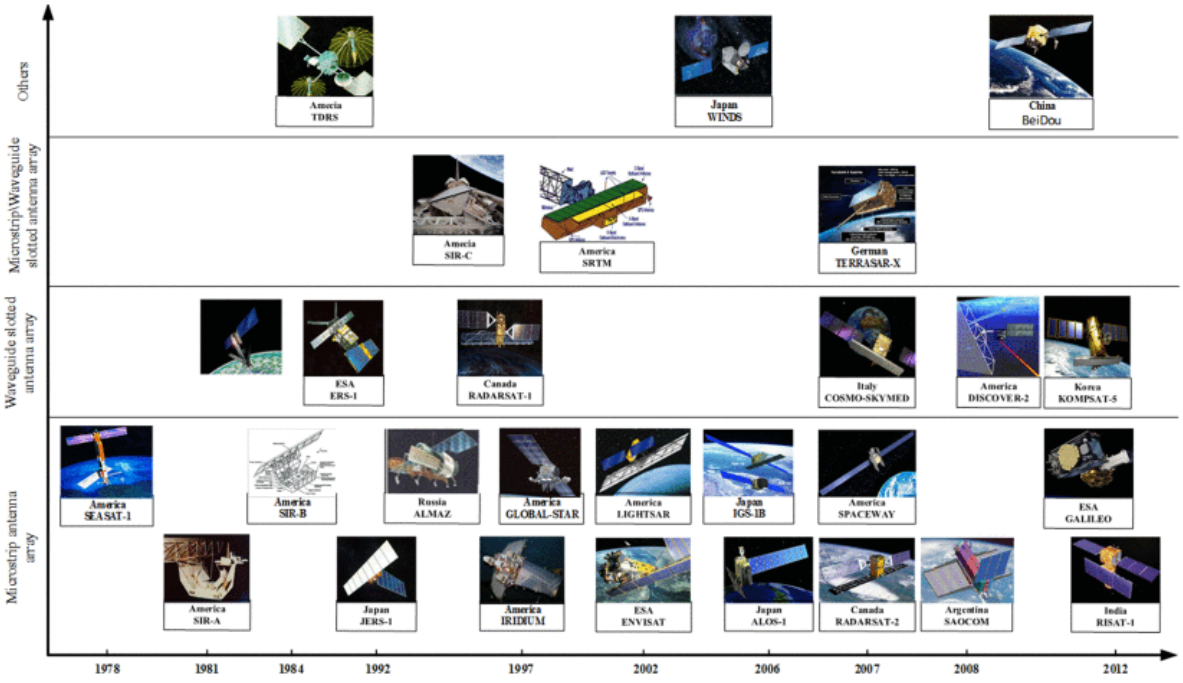

Fig. 12. Some examples of satellites equipped with active phased array antennas [97].

With the continuous growing and insatiable data request, the future of phased arrays technology will face new challenges. Whereas the 5G is now under deployment, the research is focused on the implementation of 6G wireless communications with promise of data rate reaching 1 Tb/s [100]. Among the promising solutions, Terahertz (THz) communications is an enabling technology offering broad bandwidths in the 0.1 – 10 THz range. However, in comparison with microwave and mm-wave frequency bands, propagation loss in the THz regime limits even more the communication distance due to the short wavelength of radiation. Fortunately, short wavelengths present the advantage to design ultra-massive antenna systems for THz beamforming [101]-[103]. This evolution will open new needs in terms of THz characterization techniques. In particular, there is an urgent need to develop advanced OTA methods for THz frequency range with bandwidths of hundreds of GHz [104].

REFERENCES

[1] P. K. Bondyopadhyay, "The first application of array antenna," *Proceedings 2000 IEEE International Conference on Phased Array Systems and Technology (Cat. No.00TH8510)*, 2000, pp. 29-32, doi: 10.1109/PAST.2000.858903.

[2] C. H. Doan, S. Emami, D. A. Sobel, A. M. Niknejad and R. W. Brodersen, "Design considerations for 60 GHz CMOS radios," in *IEEE Communications Magazine*, vol. 42, no. 12, pp. 132-140, Dec. 2004, doi: 10.1109/MCOM.2004.1367565

[3] E. Björnson, M. Bengtsson and B. Ottersten, "Optimal Multiuser Transmit Beamforming: A Difficult Problem with a Simple Solution Structure [Lecture Notes]," in *IEEE Signal Processing Magazine*, vol. 31, no. 4, pp. 142-148, July 2014, doi: 10.1109/MSP.2014.2312183.

[4] J. Li and P. Stoica, "The Phased Array Is the Maximum SNR Active Array [Lecture Notes]," in *IEEE Signal Processing Magazine*, vol. 27, no. 2, pp. 143-144, March 2010, doi: 10.1109/MSP.2009.935418.

[5] X. Gao, L. Dai, S. Han, C. I and R. W. Heath, "Energy-Efficient Hybrid Analog and Digital Precoding for MmWave MIMO Systems With Large Antenna Arrays," in *IEEE Journal on Selected Areas in Communications*, vol. 34, no. 4, pp. 998-1009, April 2016, doi: 10.1109/JSAC.2016.2549418.

[6] W. Hong *et al*., "Multibeam Antenna Technologies for 5G Wireless Communications," in *IEEE Transactions on Antennas and Propagation*, vol. 65, no. 12, pp. 6231-6249, Dec. 2017, doi: 10.1109/TAP.2017.2712819.

[7] W. Hong, K. Baek and S. Ko, "Millimeter-Wave 5G Antennas for Smartphones: Overview and Experimental Demonstration," in *IEEE Transactions on Antennas and Propagation*, vol. 65, no. 12, pp. 6250-6261, Dec. 2017, doi: 10.1109/TAP.2017.2740963.

[8] I. Ahmed *et al*., "A Survey on Hybrid Beamforming Techniques in 5G: Architecture and System Model Perspectives," in *IEEE Communications Surveys & Tutorials*, vol. 20, no. 4, pp. 3060-3097, Fourthquarter 2018, doi: 10.1109/COMST.2018.2843719.

[9] W. Fan *et al*., "A Step Toward 5G in 2020: Low-cost OTA performance evaluation of massive MIMO base stations.," in *IEEE Antennas and Propagation Magazine*, vol. 59, no. 1, pp. 38-47, Feb. 2017, doi: 10.1109/MAP.2016.2630020.

[10] W. Fan, P. Kyosti, M. Rumney, X. Chen and G. F. Pedersen, "Over-the-Air Radiated Testing of Millimeter-Wave Beam-Steerable Devices in a Cost-Effective Measurement Setup," in *IEEE Communications Magazine*, vol. 56, no. 7, pp. 64-71, July 2018, doi: 10.1109/MCOM.2018.1701006.

[11] Y. Qi et al., "5G Over-the-Air Measurement Challenges: Overview," *in IEEE Transactions on Electromagnetic Compatibility*, vol. 59, no. 6, pp. 1661-1670, Dec. 2017, doi: 10.1109/TEMC.2017.2707471.

[12] C. A. Balanis, Antenna Theory - Analysis and Design, *3rd ed. John Wiley & Sons*, Inc., 2005.

[13] V. Camarchia, R. Quaglia, A. Piacibello, D. P. Nguyen, H. Wang and A. Pham, "A Review of Technologies and Design Techniques of Millimeter-Wave Power Amplifiers," *in IEEE Transactions on Microwave Theory and Techniques*, vol. 68, no. 7, pp. 2957-2983, July 2020, doi: 10.1109/TMTT.2020.2989792.

[14] P. M. Asbeck, N. Rostomyan, M. Özen, B. Rabet and J. A. Jayamon, "Power Amplifiers for mm-Wave 5G Applications: Technology Comparisons and CMOS-SOI Demonstration Circuits," *in IEEE Transactions on Microwave Theory and Techniques*, vol. 67, no. 7, pp. 3099-3109, July 2019, doi: 10.1109/TMTT.2019.2896047.

[15] P. Rocca, G. Oliveri, R. J. Mailloux and A. Massa, "Unconventional Phased Array Architectures and Design Methodologies—A Review," *in Proceedings of the IEEE*, vol. 104, no. 3, pp. 544-560, March 2016, doi: 10.1109/JPROC.2015.2512389.

[16] R. J. Mailloux, Phased Array Antenna Handbook, *2nd ed. Artech House*, 2005.

[17] D. Muirhead, M. A. Imran and K. Arshad, "A Survey of the Challenges, Opportunities and Use of Multiple Antennas in Current and Future 5G Small Cell Base Stations," *in IEEE Access*, vol. 4, pp. 2952-2964, 2016, doi: 10.1109/ACCESS.2016.2569483.

[18] X. Gu, D. Liu and B. Sadhu, "Packaging and Antenna Integration for Silicon-Based Millimeter-Wave Phased Arrays: 5G and Beyond," *in IEEE Journal of Microwaves*, vol. 1, no. 1, pp. 123-134, Jan. 2021, doi: 10.1109/JMW.2020.3032891.

[19] A. Valdes-Garcia, B. Sadhu, X. Gu, J. Plouchart, M. Yeck and D. Friedman, "Scaling Millimeter-Wave Phased Arrays: Challenges and Solutions," *2018 IEEE BiCMOS and Compound Semiconductor Integrated Circuits and Technology Symposium (BCICTS)*, 2018, pp. 80-84, doi: 10.1109/BCICTS.2018.8551062.

[20] C. Fulton, M. Yeary, D. Thompson, J. Lake and A. Mitchell, "Digital Phased Arrays: Challenges and Opportunities," *in Proceedings of the IEEE*, vol. 104, no. 3, pp. 487-503, March 2016, doi: 10.1109/JPROC.2015.2501804.

[21] B. Rupakula, S. Zihir and G. M. Rebeiz, "Low Complexity 54–63-GHz Transmit/Receive 64- and 128-element 2-D-Scanning Phased-Arrays on Multilayer Organic Substrates With 64-QAM 30-Gbps Data Rates," *in IEEE Transactions on Microwave Theory and Techniques*, vol. 67, no. 12, pp. 5268-5281, Dec. 2019, doi: 10.1109/TMTT.2019.2952579.

[22] S. S. Holland, D. H. Schaubert and M. N. Vouvakis, "A 7–21 GHz Dual-Polarized Planar Ultrawideband Modular Antenna (PUMA) Array," *in IEEE Transactions on Antennas and Propagation*, vol. 60, no. 10, pp. 4589-4600, Oct. 2012, doi: 10.1109/TAP.2012.2207321.

[23] B. Cetindogan, E. Ozeren, B. Ustundag, M. Kaynak and Y. Gurbuz, "A 6 Bit Vector-Sum Phase Shifter With a Decoder Based Control Circuit for X-Band Phased-Arrays," *in IEEE Microwave and Wireless Components Letters*, vol. 26, no. 1, pp. 64-66, Jan. 2016, doi: 10.1109/LMWC.2015.2505618.

[24] C. Quan, S. Heo, M. Urteaga and M. Kim, "A 275 GHz Active Vector-Sum Phase Shifter," *in IEEE Microwave and Wireless Components Letters*, vol. 25, no. 2, pp. 127-129, Feb. 2015, doi: 10.1109/LMWC.2014.2382655.

[25] J. Jang, B. Kim, C. Kim and S. Hong, "79-GHz Digital Attenuator-Based Variable-Gain Vector-Sum Phase Shifter With High Linearity," *in IEEE Microwave and Wireless Components Letters*, vol. 28, no. 8, pp. 693-695, Aug. 2018, doi: 10.1109/LMWC.2018.2842688.

[26] D. Hao, W. Zhang, X. Liu and Y. Liu, "A Low Insertion Loss Variation Trombone True Time Delay in GaAs pHEMT Monolithic Microwave Integrated Circuit," in *IEEE Microwave and Wireless Components Letters*, vol. 31, no. 7, pp. 889-892, July 2021, doi: 10.1109/LMWC.2021.3075990.

[27] S. Park and S. Jeon, "A 15–40 GHz CMOS True-Time Delay Circuit for UWB Multi-Antenna Systems," in *IEEE Microwave and Wireless Components Letters*, vol. 23, no. 3, pp. 149-151, March 2013, doi: 10.1109/LMWC.2013.2244872.

[28] D. -H. Shin, I. -B. Yom and D. -W. Kim, "4–20 GHz GaAs True-Time Delay Amplifier MMIC," in *IEEE Microwave and Wireless Components Letters*, vol. 27, no. 12, pp. 1119-1121, Dec. 2017, doi: 10.1109/LMWC.2017.2763754.

[29] J. W. Lee and S. Y. Kim, "60GHz switched-line-type phase shifter using body-floating switches in 0.13m CMOS technology," *in Electronic Letters*, vol. 48, no. 7, pp. 376-378, 2012, doi: 10.1049/el.2012.0001.

[30] G. D. Lynes, G. E. Johnson, B. E. Huckleberry and N. H. Forrest, "Design of a Broad-Band 4-Bit Loaded Switched-Line Phase Shifter," *in IEEE Transactions on Microwave Theory and Techniques*, vol. 22, no. 6, pp. 693-697, Jun. 1974, doi: 10.1109/TMTT.1974.1128312.

[31] J. C. S. Chieh, J. Rowland, and S. Sharma, "Four-bit W-band switched line phase shifter in 90 nm SiGe," *in Electronic Letters*, vol. 54, no. 17, pp. 1040-1041, 2018, doi: 10.1049/el.2018.5380.

[32] R. L. Schmid, A. Ç. Ulusoy, P. Song and J. D. Cressler, "A 94 GHz, 1.4 dB Insertion Loss Single-Pole Double-Throw Switch Using Reverse-Saturated SiGe HBTs," *in IEEE Microwave and Wireless Components Letters*, vol. 24, no. 1, pp. 56-58, Jan. 2014, doi: 10.1109/LMWC.2013.2288276.

[33] W. Lai, C. Chou, S. Huang, T. Huang and H. Chuang, "75–110-GHz W -band High-Linearity Traveling-Wave T/R Switch by Using Negative Gate/Body-Biasing in 90-nm CMOS," *in IEEE Microwave and Wireless Components Letters*, vol. 27, no. 5, pp. 488-490, May 2017, doi: 10.1109/LMWC.2017.2690837.

[34] T. M. Hancock and G. M. Rebeiz, "A 12-GHz SiGe phase shifter with integrated LNA," in IEEE Transactions on Microwave Theory and Techniques, vol. 53, no. 3, pp. 977-983, March 2005, doi: 10.1109/TMTT.2004.842479.

[35] A. Bautista, A. Franc and P. Ferrari, "Accurate Parametric Electrical Model for Slow-Wave CPW and Application to Circuits Design," *in IEEE Transactions on Microwave Theory and Techniques*, vol. 63, no. 12, pp. 4225-4235, Dec. 2015, doi: 10.1109/TMTT.2015.2495242.

[36] H. A. Atwater, "Circuit Design of the Loaded-Line Phase Shifter," *in IEEE Transactions on Microwave Theory and Techniques*, vol. 33, no. 7, pp. 626-634, Jul. 1985, doi: 10.1109/TMTT.1985.1133038.

[37] Z. Iskandar et al., "A 30–50 GHz reflection-type phase shifter based on slow-wave coupled lines in BiCMOS 55 nm technology," *2016 46th European Microwave Conference (EuMC)*, 2016, pp. 1413-1416, doi: 10.1109/EuMC.2016.7824618.

[38] R. Garg and A. S. Natarajan, "A 28-GHz Low-Power Phased-Array Receiver Front-End With 360° RTPS Phase Shift Range," *in IEEE Transactions on Microwave Theory and Techniques*, vol. 65, no. 11, pp. 4703-4714, Nov. 2017, doi: 10.1109/TMTT.2017.2707414.

[39] T. Li and H. Wang, "A Millimeter-Wave Fully Integrated Passive Reflection-Type Phase Shifter With Transformer-Based Multi-Resonance Loads for 360° Phase Shifting," *in IEEE Transactions on Circuits and Systems I: Regular Papers*, vol. 65, no. 4, pp. 1406-1419, April 2018, doi: 10.1109/TCSI.2017.2748078.

[40] P. Hindle, "Comprehensive Survey of Commercial mmWave Phased Array Companies," *Microwave Journal*, Jan. 2020.

[41] S. Shahramian, M. J. Holyoak, A. Singh and Y. Baeyens, "A Fully Integrated 384-Element, 16-Tile, W -Band Phased Array With Self-Alignment and Self-Test," *in IEEE Journal of Solid-State Circuits*, vol. 54, no. 9, pp. 2419-2434, Sept. 2019, doi: 10.1109/JSSC.201.

[42] B. Sadhu, X. Gu and A. Valdes-Garcia, "The More (Antennas), the Merrier: A Survey of Silicon-Based mm-Wave Phased Arrays Using Multi-IC Scaling," *in IEEE Microwave Magazine*, vol. 20, no. 12, pp. 32-50, Dec. 2019, doi: 10.1109/MMM.2019.2941632.

[43] S. Zihir, O. D. Gurbuz, A. Kar-Roy, S. Raman and G. M. Rebeiz, "60-GHz 64- and 256-Elements Wafer-Scale Phased-Array Transmitters Using Full-Reticle and Subreticle Stitching Techniques," *in IEEE Transactions on Microwave Theory and Techniques*, vol. 64, no. 12, pp. 4701-4719, Dec. 2016, doi: 10.1109/TMTT.2016.2623948.

[44] U. Kodak, B. Rupakula, S. Zihir and G. M. Rebeiz, "60-GHz 64- and 256-Element Dual-Polarized Dual-Beam Wafer-Scale Phased-Array Transceivers With Reticle-to-Reticle Stitching," *in IEEE Transactions on Microwave Theory and Techniques*, vol. 68, no. 7, pp. 2745-2767, July 2020, doi: 10.1109/TMTT.2020.2969904.

[45] X. Gu, D. Liu, C. Baks, J. Plouchart, W. Lee and A. Valdes-Garcia, "An Enhanced 64-Element Dual-Polarization Antenna Array Package for W-Band Communication and Imaging Applications," *2018 IEEE 68th Electronic Components and Technology Conference (ECTC)*, 2018, pp. 197-201, doi: 10.1109/ECTC.2018.00038.

[46] J. D. Dunworth et al., "A 28GHz Bulk-CMOS dual-polarization phased-array transceiver with 24 channels for 5G user and basestation equipment," *2018 IEEE International Solid - State Circuits Conference - (ISSCC)*, 2018, pp. 70-72, doi: 10.1109/ISSCC.2018.8310188.

[47] B. Sadhu et al., "A 28GHz 32-element phased-array transceiver IC with concurrent dual polarized beams and 1.4 degree beam-steering resolution for 5G communication," *2017 IEEE International Solid-State Circuits Conference (ISSCC)*, 2017, pp. 128-129, doi: 10.1109/ISSCC.2017.7870294.

[48] K. Kibaroglu, M. Sayginer, T. Phelps and G. M. Rebeiz, "A 64-Element 28-GHz Phased-Array Transceiver With 52-dBm EIRP and 8–12-Gb/s 5G Link at 300 Meters Without Any Calibration," *in IEEE Transactions on Microwave Theory and Techniques*, vol. 66, no. 12, pp. 5796-5811, Dec. 2018, doi: 10.1109/TMTT.2018.2854174.

[49] Y. Yin, Z. Zhang, T. Kanar, S. Zihir and G. M. Rebeiz, "A 24-29.5 GHz 256-Element 5G Phased-Array with 65.5 dBm Peak EIRP and 256-QAM Modulation," *2020 IEEE/MTT-S International Microwave Symposium (IMS)*, 2020, pp. 687-690, doi: 10.1109/IMS30576.2020.9224031.

[50] H.-C. Park et al., "Millimeter-Wave Band CMOS RF Phased-Array Transceiver IC Designs for 5G Applications," *2020 IEEE International Electron Devices Meeting (IEDM)*, 2020, pp. 17.2.1-17.2.4, doi: 10.1109/IEDM13553.2020.9371948.

[51] X. Gu et al., "A compact 4-chip package with 64 embedded dual-polarization antennas for W-band phased-array transceivers," *2014 IEEE 64th Electronic Components and Technology Conference (ECTC)*, 2014, pp. 1272-1277, doi: 10.1109/ECTC.2014.6897455.

[52] S. Pellerano et al., "A Scalable 71-to-76GHz 64-Element Phased-Array Transceiver Module with 2×2 Direct-Conversion IC in 22nm FinFET CMOS Technology," *2019 IEEE International Solid- State Circuits Conference - (ISSCC)*, 2019, pp. 174-176, doi: 10.1109/ISSCC.2019.8662496.

[53] A. Pallotta et al., "SiGe:BiCMOS technology is enabling D-band link with Active Phased Antenna Array," *in 2021 Joint European Conference on Networks and Communications 6G Summit (EuCNC/6G Summit)*, 2021, pp. 496 501, doi: 10.1109/EuCNC/6GSummit51104.2021.9482432.

[54] T. Sowlati et al., "A 60-GHz 144-Element Phased-Array Transceiver for Backhaul Application," *in IEEE Journal of Solid-State Circuits*, vol. 53, no. 12, pp. 3640-3659, Dec. 2018, doi: 10.1109/JSSC.2018.2874048.

[55] H. Wheeler, "Simple relations derived from a phased array made of an infinite current sheet," *1964 Antennas and Propagation Society International Symposium*, 1964, pp. 157-160, doi: 10.1109/APS.1964.1150148.

[56] A. Neto, D. Cavallo, G. Gerini and G. Toso, "Scanning Performances of Wideband Connected Arrays in the Presence of a Backing Reflector," *in IEEE Transactions on Antennas and Propagation*, vol. 57, no. 10, pp. 3092-3102, Oct. 2009, doi: 10.1109/TAP.2009.2028631.

[57] D. Cavallo, A. Neto, G. Gerini, A. Micco and V. Galdi, "A 3- to 5-GHz Wideband Array of Connected Dipoles With Low Cross Polarization and Wide-Scan Capability," *in IEEE Transactions on Antennas and Propagation*, vol. 61, no. 3, pp. 1148-1154, March 2013, doi: 10.1109/TAP.2012.2231920.

[58] R. Bolt, G. Cavallo D. Gerini, D. Deurloo, R. Grooters, A. Neto, and G. Toso, "Characterization of a dual-polarized connected-dipole array for Ku- band mobile terminals," *IEEE Transaction on Antennas and Propagation*, vol. 64, no. 2, 2016, doi: 10.1109/TAP.2015.2509505.

[59] D. Cavallo, W. Syed, and A. Neto, "Connected-slots array with artificial dielectric: A 6 to 15 GHz dual-pol wide-scan prototype," *IEEE Transaction on Antennas and Propagation*, vol. 66, no. 6, 2018, doi: 10.1109/TAP.2018.2811841.

[60] A. Van Katwijk, A. Neto, G. Toso, and D. Cavallo, "Design of wideband wide-scanning dual-polarized phased array covering simultaneously both the Ku- and the Ka-SatCom bands," *EuCAP*, 2020, doi: 10.23919/EuCAP48036.2020.9135541.

[61] D. Cavallo, A. Neto and G. Gerini, "Analysis of common-mode resonances in arrays of connected dipoles and possible solutions," 2009 European Radar Conference (EuRAD), 2009, pp. 441-444.

[62] B. Munk et al., "A low-profile broadband phased array antenna," IEEE Antennas and Propagation Society International Symposium. Digest. Held in conjunction with: USNC/CNC/URSI North American Radio Sci. Meeting (Cat. No.03CH37450), 2003, pp. 448-451 vol.2, doi: 10.1109/APS.2003.1219272.

[63] J. Doane, K. Sertel, and J. Volakis, "A wideband, wide scanning tightly coupled dipole array with integrated balun (TCDA-IB)," *IEEE Transaction on Antennas and Propagation*, vol. 61, no. 9, 2013, doi: 10.1109/TAP.2013.2267199.

[64] M. Novak and J. Volakis, "Ultra-wideband antennas for multiband satellite communications at UHF-Ku frequencies," *IEEE Transaction on Antennas and Propagation*, vol. 63, no. 4, 2015, doi: 10.1109/TAP.2015.2390616.

[65] E. Yetisir, N. Ghalichechian, and J. Volakis, "Ultra-wideband array with 70° scanning using FSS superstrate," *IEEE Transaction on Antennas and Propagation*, vol. 64, no. 10, 2016, doi: 10.1109/TAP.2016.2594817.

[66] M. Novak, F. Miranda, and J. Volakis, "Ultra-wideband phased array for millimetre wave ism and 5G bands, realized in PCB," *IEEE Transaction on Antennas and Propagation*, vol. 66, no. 12, 2018, doi: 10.1109/TAP.2018.2872177.

[67] A. D. Johnson, J. Zhong, S. B. Venkatakrishnan, E. A. Alwan, and J. L. Volakis, "Phased array with low angle scanning and 46:1 bandwidth," *IEEE Transactions on Antennas and Propagation*, 2020, doi: 10.1109/TAP.2020.2998869.

[68] A. D. Johnson, J. Zhong, S. Sekelsky, E. A. Alwan, and J. L. Volakis, "Dual-polarised wideband tightly coupled dipole array for airborne applications," *IET Microwaves, Antennas Propagation*, vol. 14, no. 12, 2020, doi: 10.1109/APS.2015.7305389.

[69] M. Vouvakis and S. Holland, "The planar Ultra-wideband modular antenna (PUMA) array," *IEEE Transaction on Antennas and Propagation*, vol. 60, no. 1, 2012, doi: 10.1109/TAP.2011.2167916.

[70] 24 S. Holland, D. Schaubert, and M. Vouvakis, "A 7–21 GHz dual-polarized planar Ultra-wideband modular antenna (PUMA) array," *IEEE Transaction on Antennas and Propagation*, vol. 60, no. 10, 2012, doi: 10.1109/TAP.2012.2207321.

[71] T. Logan, R. Kindt, M. Lee, and M. Vouvakis, "A new class of planar Ultra-wideband modular antenna arrays with improved bandwidth," *IEEE Transaction on Antennas and Propagation*, vol. 66, no. 2, 2018, doi: 10.1109/TAP.2017.2780878.

[72] W. Milroy, "Continuous transverse stub element devices and methods of making same," *U.S. Patent 5 266 961*, 1993.

[73] M. Ettorre, F. Manzillo, M. Casaletti, R. Sauleau, L. Le Coq, and N. Capet, "Continuous transverse stub array for Ka-band applications," *IEEE Transaction on Antennas and Propagation*, vol. 63, no. 11, 2015, doi: 10.1109/TAP.2015.2479243.

[74] W. Milroy, "Continuous transverse stub element antenna arrays using voltage-variable dielectric material," *United States Patent Brevet 5,583,524*, 1996.

[75] F. Foglia Manzillo *et al*., "A wide-angle scanning switched-beam antenna system in LTCC technology with high beam crossing levels for V-band communications," *IEEE Transactions on Antennas and Propagation*, vol. 67, no. 1, pp. 541-553, Jan. 2019, doi: 10.1109/TAP.2018.2877467.

[76] T. Potelon, M. Ettorre, L. Le Coq, T. Bateman, J. Francey, and R. Sauleau, "Reconfigurable CTS antenna fully integrated in PCB technology for 5g backhaul applications," *IEEE Transaction on Antennas and Propagation*, vol. 67, no. 6, 2019, doi: 10.1109/TAP.2019.2902644.

[77] Rohde and Schwarz, "Antenna Array Testing - Conducted and Over the Air: The Way to 5G," *White Paper*, 2017.

[78] The 3rd Generation Partnership Project (3GPP TM), "Base Station (BS) conformance testing 38.141-2," *3rd Generation Partnership Project*, 2020.

[79] The 3rd Generation Partnership Project (3GPP TM), "User Equipment (UE) conformance specification 38.512-2," *3rd Generation Partnership Projec*t, 2020.

[80] CTIA Certification Program, "Test Plan for Wireless Device Over-the-Air Performance," *CTIA Certification Program*, 2020.

[81] The 3rd Generation Partnership Project (3GPP TM), "38.810 Technical Specification Group Radio Access Network NR Study on Test Methods," 2019

[82] The 3rd Generation Partnership Project (3GPP TM), "38.101-2 Evolved Universal Terrestrial Radio Access (E-UTRA) User Equipment (UE) conformance specification Radio transmission and reception Part 1: Conformance testing," 2011.

[83] National Instruments, "Performing System Calibration", online manual: https://www.ni.com/documentation/en/mmwave-ota-validation-test-reference-architecture/latest/user-manual/perform-system-calibration/

[84] Keysight Technologies, "On Coarse & Fine TX Beam Peak Search Measurement Approaches," 2018

[85] M. Bagget, D. Dorent, Hess, "Power Handling Considerations in a Compact Range," in 35th Annual Meeting and Symposium of Antenna Measurement Techniques Association, Columbus Ohio, 2013.

[86] The 3rd Generation Partnership Project (3GPP TM), "38.903 Derivation of test tolerances and measurement uncertainty for User Equipment (UE) conformance test cases," 2019

[87] A. Weiss, J. Quimby , R. Leonhardt , B. Jamroz , D. Williams , K. Remley , P. Vouras, and A. Elsherbeni. Setup and Control of a Millimeter-Wave Synthetic Aperture Measurement System with Uncertainties. Paper presented Aug. 7, 2020, at the 95th ARFTG Microwave Measurement Conference

[88] I. Ahmed et al., "A Survey on Hybrid Beamforming Techniques in 5G: Architecture and System Model Perspectives," in IEEE Communications Surveys & Tutorials, vol. 20, no. 4, pp. 3060-3097, Fourthquarter 2018, doi: 10.1109/COMST.2018.2843719.

[89] Z. Pi, J. Choi and R. Heath, "Millimeter-wave gigabit broadband evolution toward 5G: fixed access and backhaul," in *IEEE Communications Magazine*, vol. 54, no. 4, pp. 138-144, April 2016, doi: 10.1109/MCOM.2016.7452278.

[90] Z. Pi and F. Khan, "An introduction to millimeter-wave mobile broadband systems," in *IEEE Communications Magazine*, vol. 49, no. 6, pp. 101-107, June 2011, doi: 10.1109/MCOM.2011.5783993.

[91] T. L. Marzetta, "Noncooperative Cellular Wireless with Unlimited Numbers of Base Station Antennas," in *IEEE Transactions on Wireless Communications*, vol. 9, no. 11, pp. 3590-3600, November 2010, doi: 10.1109/TWC.2010.092810.091092.

[92] N. Bhushan *et al*., "Network densification: the dominant theme for wireless evolution into 5G," in *IEEE Communications Magazine*, vol. 52, no. 2, pp. 82-89, February 2014, doi: 10.1109/MCOM.2014.6736747.

[93] P. Choi, D. A. Antoniadis and E. A. Fitzgerald, "Towards Millimeter-Wave Phased Array Circuits and Systems For Small Form Factor and Power Efficient 5G Mobile Devices," 2019 IEEE International Symposium on Phased Array System & Technology (PAST), 2019, pp. 1-5, doi: 10.1109/PAST43306.2019.9021005.

[94] W. Roh, et al., "Millimeter-wave beamforming as an enabling technology for 5G cellular communications: Theoretical feasibility and prototype results," IEEE Communications Magazine, vol. 52, no. 2, pp. 106–113, Feb. 2014, doi: 10.1109/MCOM.2014.6736750.

[95] W. El-Halwagy, A. Nag, P. Hisayasu, F. Aryanfar, P. Mousavi, and M. Hossain, "A 28GHz quadrature fractional-N synthesizer for 5G mobile communication with less than 100fs jitter in 65nm CMOS," *in Proceedings of* IEEE Radio Frequency Integrated Circuits Symposium *(RFIC)*, May 2016, pp. 118–121, doi: 10.1109/RFIC.2016.7508265.

[96] W. Townsend, "An initial assessment of the performanceachieved by the SEASAT-1 radar altimeter," *IEEE Journal of Oceanic Engineerin, g*,vol. 5, no. 2, pp. 80–92, 1980, doi: 10.1109/JOE.1980.1145459.

[97] S. Buckreuss, U. Steinbrecher and B. Schättler, "The TerraSAR-X mission status," *2015 IEEE 5th Asia-Pacific Conference on Synthetic Aperture Radar (APSAR)*, 2015, pp. 357-361, doi: 10.1109/APSAR.2015.7306224.

[98] S. Srivastava, S. Cote, S. Muir and R. Hawkins, "The RADARSAT-1 imaging performance, 14 years after launch, and independent report on RADARSAT-2 image quality," *2010 IEEE International Geoscience and Remote Sensing Symposium*, 2010, pp. 3458-3461, doi: 10.1109/IGARSS.2010.5650129.

[99] C. Wang *et al*., "Space Phased Array Antenna Developments: A Perspective on Structural Design," in *IEEE Aerospace and Electronic Systems Magazine*, vol. 35, no. 7, pp. 44-63, 1 July 2020, doi: 10.1109/MAES.2020.2984300.

[100] C. Han, L. Yan and J. Yuan, "Hybrid Beamforming for Terahertz Wireless Communications: Challenges, Architectures, and Open Problems," in *IEEE Wireless Communications*, vol. 28, no. 4, pp. 198-204, August 2021, doi: 10.1109/MWC.001.2000458.

[101] H. Sarieddeen, M. -S. Alouini and T. Y. Al-Naffouri, "Terahertz-Band Ultra-Massive Spatial Modulation MIMO," in *IEEE Journal on Selected Areas in Communications*, vol. 37, no. 9, pp. 2040-2052, Sept. 2019, doi: 10.1109/JSAC.2019.2929455.

[102] T. Sun *et al*., "Terahertz Beam Steering based on CMOS Tunable Metamaterials," *2021 46th International Conference on Infrared, Millimeter and Terahertz Waves (IRMMW-THz)*, 2021, pp. 1-2, doi: 10.1109/IRMMW-THz50926.2021.9567412.

[103] K. Okada, "CMOS THz Phased-Array Transceivers for Beyond 5G," *2021 IEEE International Symposium on Radio-Frequency Integration Technology (RFIT)*, 2021, pp. 1-2, doi: 10.1109/RFIT52905.2021.9565313.

[104] C. De Martino, A. Visweswaran and M. Spirito, "Over-the-Air Characterization Of mm-Wave On-Chip Antennas and Tx Modules, Concept and Calibration," *2020 95th ARFTG Microwave Measurement Conference (ARFTG)*, 2020, pp. 1-4, doi: 10.1109/ARFTG47271.2020.9241375.